(12)

SC5325.1PR

SC5325.1PR

Copy No. 20

STUDY PROCESSING OF CERAMIC MATERIAL

PROGRESS REPORT NO. 1 FOR THE PERIOD
April 1982 through January 1983

CONTRACT NO. N00014-82-C-0341

Prepared for

Material Sciences Division
Office of Naval Research
800 N. Quincy Street
Arlington, VA 22217

F.F. Lange
Principal Investigator

JANUARY 1983

Approved for public release; distribution unlimited

Rockwell International
Science Center

respect to the size of the multiple-particle packing unit, consolidation forces and phenomena develop during sintering.

One pertinent conclusion is that the multiple-particle packing units, density and support grain growth as sintering initiates. Grain growth and rearrangement processes decreases the coordination number of remaining pores to allow them to disappear during latter states of sintering. Porosimetry and direct observations of powder compacts of < 1 μm Al_2O_3 heat treated between 600°C and 1600°C are consistent with this concept.

TABLE OF CONTENTS

Page

1.0 INTRODUCTION..... 1

2.0 THE PORE COORDINATION NUMBER DISTRIBUTION..... 3

3.0 EXPERIMENTAL..... 16

4.0 RESULTS..... 17

4.1 Bulk Density and Intrusion Capillaries..... 17
4.2 Microstructural Observations..... 17

5.0 DISCUSSION..... 27

6.0 REFERENCES..... 29

LIST OF FIGURES

Figure		Page
Fig. 1	Surface curvature for two pores with the same approximate volume and dihedral angle, but with coordinating grains numbers larger (a) and smaller (b) than R_c	4
Fig. 2	Schematic of packed agglomerates	8
Fig. 3	Schematic of the pore coordination number distribution of an agglomerated powder indicating the three classes of pores: pores within domains, between domains and between agglomerates	9
Fig. 4	End-point density of a ZrO_2/y_2O_3 powder sintered at either 1700°C or 1850°C as a function of initial bulk density	11
Fig. 5	Bulk density vs temperature (30 min soak) for < 1 μm α-Al_2O_3, dispersed, flocced, casted into a plastic mold and evaporated prior to heating	18
Fig. 6	Equivalent capillary size for mercury intrusion at different sintering temperatures (30 min scale) vs volume of intruded mercury	19
Fig. 7	Polished microstructure of < 1 μm α-Al_2O_3 sintered at 1200°C/30 min. a) as-polished, b) pores blanched, c) size distribution of pores	20
Fig. 8	Unpolished surface of < 1 μm α-Al_2O_3 sintered at 800°C/30 min: a) shows interconnected agglomerates (cross marks for relocation) and b) shows interconnected domains (see box in a)	23
Fig. 9	Series of SEM observations of same surface area of < 1 μm Al_2O_3 sintered at temperatures indicated for 30 min	25
Fig. 10	(Same as Fig. 9) - Note change of agglomerate shape during grain growth	26

SINTERABILITY OF AGGLOMERATED CERAMIC POWDERS

By

F. F. Lange

Rockwell International Science Center
Thousand Oaks, CA 91360

ABSTRACT

A concept is presented which relates the sinterability of a powder compact to its particle arrangement as defined by the distribution of pore coordination numbers, i.e., the number of touching particles surrounding and defining each void space.

Previous thermodynamic arguments suggest that pores will only disappear when their coordination number is less than a critical value. The coordination number distribution of an agglomerated powder is discussed with respect to the size of the multiple-particle packing unit, consolidation forces and phenomena develop during sintering.

One pertinent conclusion is that the multiple-particle packing units, density and support grain growth as sintering initiates. Grain growth and rearrangement processes decreases the coordination number of remaining pores to allow them to disappear during latter states of sintering. Porosimetry and direct observations of powder compacts < 1 μm Al_2O_3 heat treated between 600°C and 1600°C are consistent with this concept.

1.0 INTRODUCTION

Sintering theories and 'validating' experiments have primarily emphasized material transport mechanisms and kinetics. Most of these theories are based on simple particle shapes (viz spheres) and simple particle arrangements (e.g., two spheres). Although experiments conducted with these simple shapes and arrangements have been very instructive, Exner[1] concludes that "... any conclusions drawn by comparing these theoretical approaches with experiments on particles of unequal size in irregular arrangements or in real powders must be regarded with the greatest caution."

Ceramic powders are known to contain agglomerates. Agglomerates can be classified as either hard, i.e., partially sintered or cemented groups of particles, or soft, i.e., groups held together by van der Waals forces and easily broken apart with surfactants. All dry, fine particle size (< 10 μm) ceramic powders can be expected to contain soft agglomerates.

Haberko[2] has shown that water washed ZrO_2-Y_2O_3 gels produce hard agglomerates, whereas further washing with ethyl alcohol produces soft agglomerates. For a given consolidation pressure, the soft agglomerated powder packs with a lower bulk density relative to the hard agglomerated powder (e.g., both powders calcined at 500°C, $\rho_s = 0.31\ \rho_t$, and $\rho_h = 0.41\ \rho_t$; calcined at 1000°C, $\rho_s = 0.40\ \rho_t$, $\rho_h = 0.51\ \rho_t$).* Despite its lower bulk density, the end-point density at 1300°C/3 hrs of the soft agglomerated powder is $> 0.98\ \rho_t$, whereas the hard agglomerated powder ranges between $0.82\ \rho_t$ and $0.86\ \rho_t$, depending on the calcining temperature. Haberko explains these results by suggesting that the soft agglomerated powder packs more uniformity.

Neisz and Bennett[3] have shown that laundering Al_2O_3 powder results in fewer hard agglomerates and improves sinterability. Reed et al[4] also conclude that agglomerates ". . . greatly affect the evolution of microstructure and

---

* ρ is density, s, h, t denotes soft, hard and theoretical, respectively.

ultimate temperatures and grain sizes required for densification, . . ." Bruch[5] and others have shown that bulk density, a reflection of particle arrangement, strongly influences sinterability and sintering kinetics. Judging these and other results, one must conclude that particle arrangement, a parameter neglected by theorists and many experimentalists, influences sinterability.

The purpose of the present paper is to examine particle arrangements in terms of how groups of highly coordinated particles might pack together to form pores, which can be characterized by the number of coordinating particles. This representation is instructive since a pore's coordination number determines whether or not it can eventually disappear by mass transport. Factors that govern the coordination number distribution during both powder consolidation and sintering will be discussed.

Observations will then be presented for a Al_2O_3 powder describing its evolving microstructure during sintering. It will be shown that the small packing units densify and support grain growth prior to bulk shrinkage. One interesting conclusion is that grain growth during sintering is necessary to reduce the coordination number of some voids, and to thus achieve an end-point density approaching theoretical.

2.0 THE PORE COORDINATION NUMBER DISTRIBUTION

The purpose of sintering is to eliminate the void space in a consolidated powder. Although a powder's void space is interconnecting, one can visualize this space as divided into separate entities or pores, each being bounded by a 'surface' of touching particles. In this way, each pore has a size, shape and coordination number. The coordination number is simply the number of touching particles which bound the 'surface' of the pore.

If the contacting particles are not disrupted during heating, direct observations have shown that the touching particles will first develop bridging necks (e.g., see Ref. 1). Theory, backed by direct observation, shows that neck formation in crystalline powders can occur by either evaporation and condensation or diffusional processes (surface, volume and/or grain boundary). Once necks form, further mass rearrangement occurs in an attempt to produce a pore surface morphology that is determined by the dihedral angle* and the pore's coordination number. Figure 1 illustrates the morphologies for two pores of the same volume, but with different coordination numbers. The dihedral angle is the same for both pores. Looking from within the pore, the pore with the higher coordination number has convex surfaces, whereas the surfaces of the one with the lower coordination number are concave. In general, for a given dihedral angle, a critical coordination number, R_c, exits that defines the transition from convex ($R > R_c$) to concave ($R < R_c$) surfaces.

Kingery and Francois[6] were the first to recognize that only those pores with $R < R_c$ would be able to disappear during sintering. They argued that pore shrinkage required matter to diffuse from grain boundaries to the pore surface. This diffusional process is driven by the differential chemical potential of matter at the boundary and at the pore surface. Since the sign

* The dihedral angle is defined as $\cos(\phi/2) = \gamma_{gb}/2\gamma_s$, where γ_{gb} = the grain boundary energy per unit area, and γ_s = the pore surface energy per unit area.

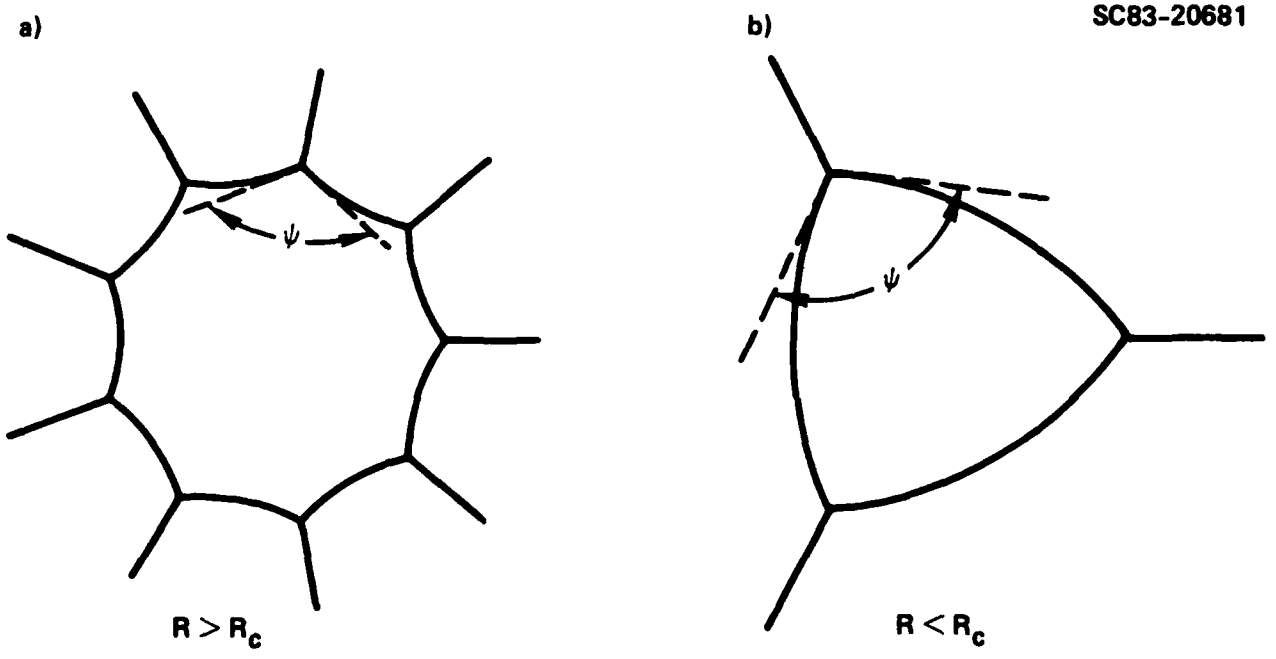

Fig. 1 Surface curvature for two pores with the same approximate volume and dihedral angle, but with coordinating grains numbers larger (a) and smaller (b) than R_c.

of the differential chemical potential depends on the surface curvature of the pore surface relative to the flat grain boundary, then concluded that material will only diffuse to the pore surface when $R < R_c$. Kingery and Francois also concluded that pores with $R > R_c$ will grow. A more recent and rigorous analysis by Cannon[7] has shown that all pores will initially undergo some shrinkage after necking, but only those with $R < R_c$ will have the thermodynamic potential to disappear. Cannon shows that pores with $R > R_c$ will shrink to an equilibrium size, and thus limit the end-point density to less than theoretical. Kingery and Francois determined the critical coordination number as a function of the dihedral angle, i.e., R_c increases with ϕ.

Let us now couple the idea of a critical coordination number with the likely coordination number distribution within a powder compact. A convenient representation of pores with different coordination numbers would be a function relating the volume fraction of pores in terms of their coordination number, $V_p(R)$. The total volume fraction of pores is

$$V_T = \int_4^\infty V_p(R)dR \quad , \tag{1}$$

where the lowest coordination number is assumed to be 4 (defined by four touching spheres). It should be noted that both large and small pores can have the same coordination number. This is a convenient representation, since if we know $V_p(R)$ and R_c, we can easily determine the volume fraction of pores that can disappear during sintering:

$$\int_4^{R_c} V_p(R)dR \quad ,$$

and the volume fraction which will only shrink to some equilibrium size:

$$\int_{R_c}^\infty V_p(R)dR \quad .$$

We now ask: What are the likely distribution functions for consolidated powders?

For a powder consisting of equi-sized spheres consolidated to produce a simple cubic arrangement, all pores have a coordination number of 8; thus, $V_T = V_p(8) = 0.48$. Further consolidation of the spheres to a face centered cubic (FCC) arrangement produces two types of pores, viz. small pores with R = 4 ($V_p(4) = 0.07$), and large pores with R = 6 ($V_p(6) = 0.19$) such that $V_T = 0.26$.

Radome packing of spheres large enough not to be influenced by van der Waal's attractive forces always results in $V_T = 0.37$ to 0.41. The coordination distribution for the random arrangements has received considerable attention. As detailed by Bernal,[8] and more recently by Frost,[9] the spheres and their coordinating void spaces can be replaced by certain types of deltrahedra (polyhedra with triangles for all faces) which fill space. Frost's analysis shows that a large fraction of the pores have a coordination number > 12. These pores are flat or elongated; and no unit sphere could be placed within them. The pore fraction with R > 12 depends on the center to center distance chosen for the calculation. For a center to center distance of 1.3 D (D = sphere size), $V_p(R > 12) = 0.20\ V_T$; for 1.2 D, $V_p(R > 12) = 0.60\ V_T$. Extrapolation* to a center to center distance of D (i.e., the strictest definition of a pore) indicates that most of the pores (> $0.90\ V_T$) in a randome pack of spheres have a coordination number > 12.

It is well known that when different fractions of different size spheres are packed at random, one can obtain bulk densities up to $0.95\ \rho_t$.[10] Here, the next smaller spheres partially fill the void space of the next larger spheres, and so on. Although void coordination statistics have not been determined, one must conclude that such a system of spheres not only reduces the void volume, but must also reduce the average coordination number.

---

* The analyses have not been carried out for a center to center distance < 1.2D, since it would produce relatively few coordinating deltrahedra.

Current powders used for ceramic processing are neither monodispersed nor spherical. Despite their wide distribution of particle size, tap densities rarely exceed 0.30 ρ_t, and different consolidation routes rarely produce bulk densities > 0.60 ρ_t. It is generally believed that agglomerates limit the bulk density. One can imagine that such powders are packed as agglomerates as illustrated in Fig. 2. Hunter[11] and co-workers, who have studied the rheology of agglomerated systems produced by the flocculation of colloidal dispersions, have shown that agglomerates themselves are made up of smaller and more densely packed sub-units, which we will call domains. Domains pack together to form agglomerate. Their packing arrangement is similar to that shown in Fig. 2. Using these two types of packing units, one can visualize three classes of pores: 1) pores of lowest coordination between the particles which make up the domains, 2) pores of higher coordination located between the domains, and 3) pores of still higher coordination located between the agglomerates. This classification is schematically shown in the $V_p(R)$ vs R plot of Fig. 3.

Let us now examine the effects of bulk density and the size of the multiple particle packing units (domains and agglomerates) on the coordination distribution. The effect of consolidation force on increasing the bulk density will depend on the resistance of each unit to deformation. For example, the coordinating deltrahedra of a randome packed, mono-dispersed spherical (large diameter) powder can be sheared to increase the bulk density from 0.59 ρ_t to 0.65 ρ_t,[1,12] but further consolidation requires the plastic deformation of the spheres themselves (common for metal powders). For the case of agglomerated powders, one can again draw on rheology studies of flocculated systems. Hunter[11] and co-workers have shown that as the shear stress is increased, agglomerates are the first multiple packing units to shear apart into their smaller domains. At higher shear stresses, the domains separate into their constituent particles. Using this same ordering, one might expect that an applied consolidation force would first cause the agglomerates to deform via the rearrangement of their constituent domains. That is, the domains would attempt to fill the interagglomerate pores. Higher consolidation forces would

SC83-20686

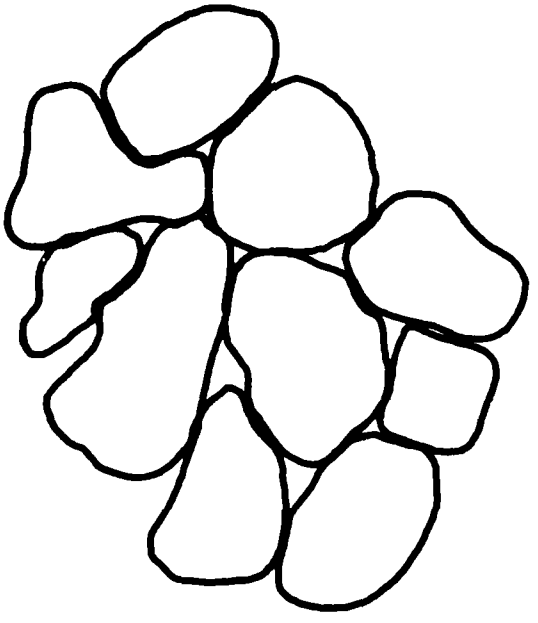

Fig. 2 Schematic of packed agglomerates.

SC83-20682

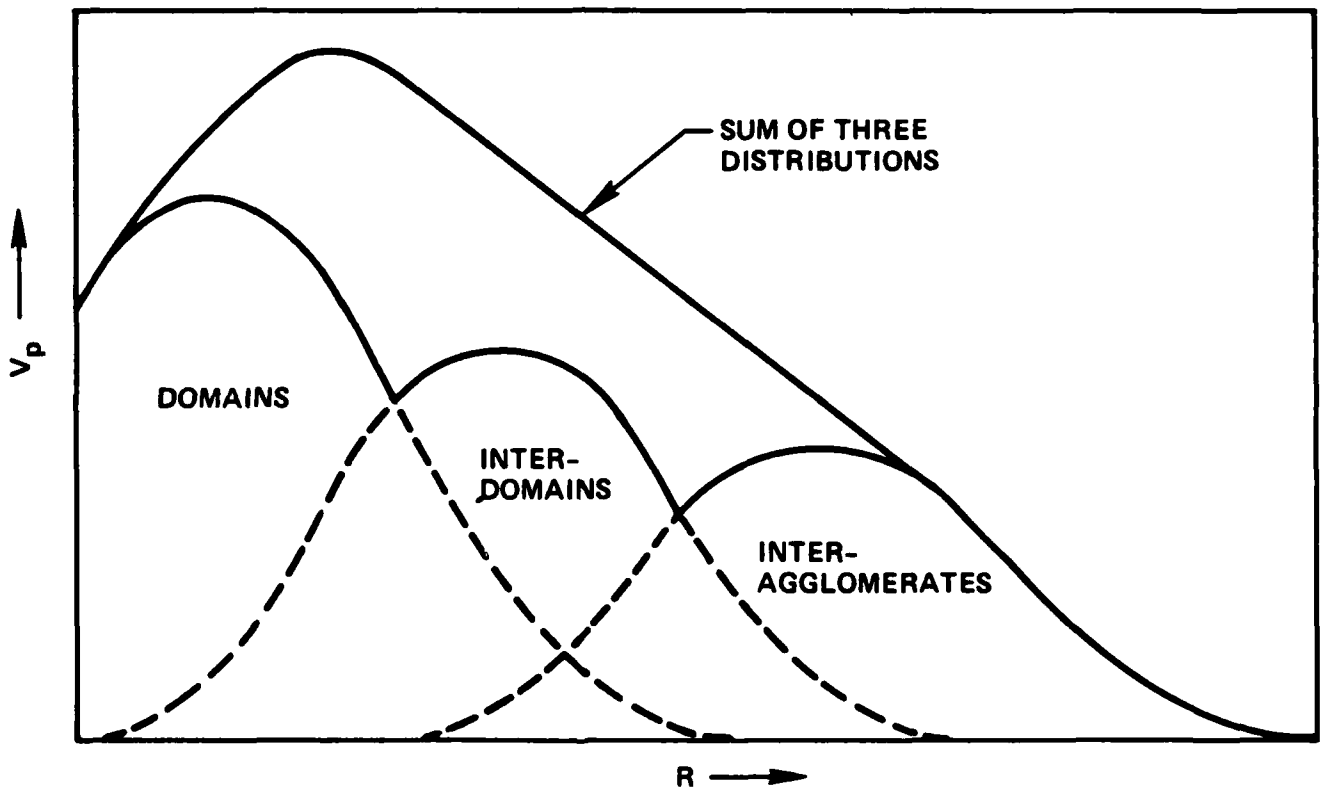

Fig. 3 Schematic of the pore coordination number distribution of an agglomerated powder indicating the three classes of pores: pores within domains, between domains and between agglomerates.

produce domain deformation via particle rearrangement, viz. particles would attempt to fill interdomain pores. Still higher forces would deform (or fracture) particles to fill the pores within the domains. Using this descriptive view, one would expect consolidation forces to increase bulk density by progressively eliminating the most highly coordinated pores. It should be noted here that if the agglomerates (or domains) are hard (partially sintered, cemented, etc.), fracture or deformation processes must be involved in the consolidation scheme.

The size of the multiple particle packing unit will also influence the coordination distribution when the bulk density is fixed. This can be illustrated by fixing the arrangement of the agglomerates, e.g., spherical agglomerates arranged on an FCC lattice. The volume fraction of pores, both within and between the agglomerates, is independent of the agglomerate size. But, since the size of the interagglomerate pores will scale with the agglomerate siz, so will their coordination number. That is, the coordination number of the interagglomerate pores will decrease with decreasing agglomerate size without changing their volume contribution to the total void volume.

Thus, the coordination distribution of an agglomerate will depend on the bulk density and the size distribution of the multiple particle packing units. Pores of a higher coordination number can be eliminated by increasing bulk density and/or decreasing the packing unit size.

Let us now examine those phenomena that might alter the coordination distribution during the sintering process. Three phenomena might be expected to alter the coordination distribution during densification: 1) pore disappearance, 2) grain growth, and 3) pore size redistribution.

As discussed above, all pores with $R < R_c$ have the opportunity to disappear, kinetics permitting. If this opportunity is permitted, and if no microstructural reorganizaton occurred during heating, then the only change expected for the coordination distribution is that all pores with $R < R_c$ will disappear. Pores with $R > R_c$ will remain to limit the end-point density $< \rho_t$. Ample evidence exists (e.g., see Fig. 4) showing that for a fixed

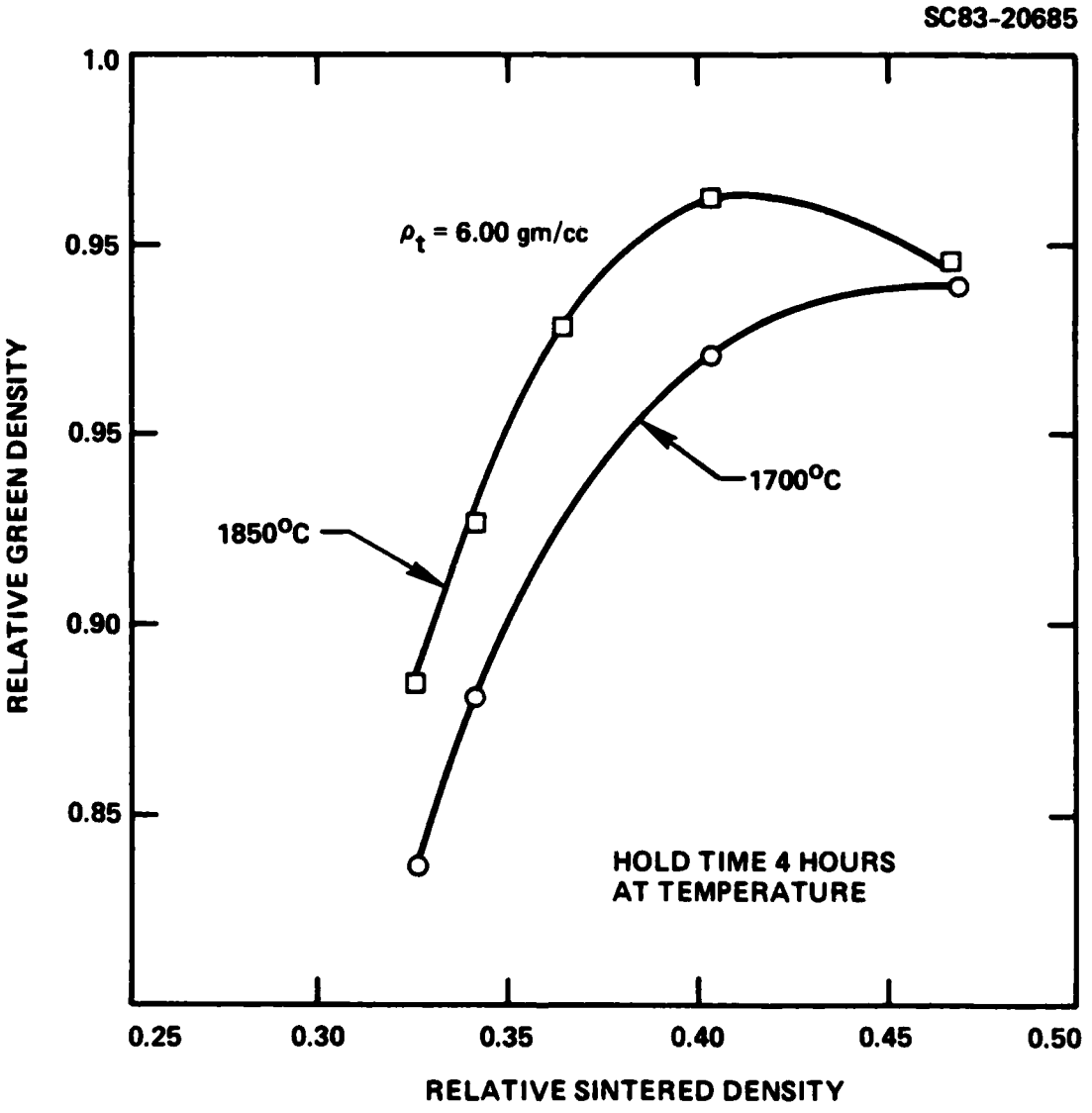

Fig. 4 End-point density of a ZrO_2/y_2O_3 powder sintered at either 1700°C or 1850°C as a function of initial bulk density.

sintering temperature and time, the end-point density is proportional to the bulk density of the powder compact.[5,13] This information is consistent with the previous argument that increasing bulk density will decrease the volume fraction of voids with the highest coordination numbers. Thus, it is reasonable to conclude that some voids within a powder compact can have a coordination number, $> R_c$, and that the volume fraction of these voids will be inversely proportional to the initial bulk density of the powder compact.

The question now becomes: For a given bulk density, what reasonable microstructural change could be induced during sintering to eliminate pores with $R > R_c$? Grain growth would be an effective microstructural change that would reduce the coordination number. That is, if the rate of grain growth exceeds the rate of pore growth, a temperature (or time) must be achieved that would reduce the coordination of all remaining voids to $< R_c$. Grain growth is known to occur through all stages of sintering. Gupta[14] has shown, for a number of different powders, that bulk density, after some sintering schedule, is proportional to grain size. Since voids are effective in preventing grain growth, one must conclude that grain growth will only occur in those volume elements that are fully (or nearly) dense, i.e, volume elements (e.g., domains and agglomerates) where $R < R_c$. Namely, as the dense regions support grain growth, the coordination number of the voids between these regions will decrease. This reasoning leads one to conclude that grain growth during sintering may be necessary* and that grain growth kinetics will, in part, control sintering kinetics. The higher end-point densities achieved at 1850°C relative to 1700°C, shown in Fig. 4, could be interpreted in this manner.

Pore size redistribution is a microstructural change that can either decrease or increase the coordination number. A smaller coordination number

---

* Many readers may find this statement repugnant, since they have been taught to avoid exaggerated grain growth that entraps pores. Entrapped pores limit the end-point density dur to kinetic reasons and must be avoided under this new concept too.

can be achieved when flat and/or elongated pores can undergo morpholgical changes ascribed to interfacial (Rayleigh) instability. This instability produces many smaller pores with the same integrated volume as the initial larger pore. This phenomena has been observed prior to the healing of large cracks (a special pore shape) introduced into polycrystalline materials by thermal shock.[15,16] Thus, for pores with special shapes, morphological changes can occur to produce smaller pores with a smaller coordination number.

A higher coordination number results when pore growth exceeds grain growth. Although several different mechanisms can be visualized which lead to this result during the latter stage of sintering (e.g., pore coalescence), discussion will be limited to a phenomena that initiates with neck growth. This phenomena is the development of separations between the multiple particle packing units. These separations, termed fissures by Vasilos and Rhodes,[13] are observed by polishing the partially sintered materials after sufficient densification to allow the specimen to be polished without disruption, but prior to reaching a density > 0.90 ρ_t. Exner,[1] who classifies this phenomena as rearrangement, has shown with planar, random arrangements of spheres, that separations develop between groups of more highly coordinated spheres (i.e., groups contain lower coordinated pores). These separations occur during neck growth. Necks that initially joined groups that shrink upon themselves can be ruptured. This process eventually results in a random array of interconnected denser regions which are 'separated' by an array of interconnected, large pores. Although some bulk shrinkage can occur during this process, the void space defining the separations grow by 'absorping' the void space within the densifying groups. Exner's remarkable experiments certainly explain the fissures obdserved by Vasilos and Rhodes and others. They also explain the mercury poresimeter results of Whittemore,[17] who showed that pores in a variety of powders can grow prior to any bulk shrinkage, and/or as bulk shrinkage initiates.

Exner's results clearly show that pores with a large coordination number can both increase in size and develop an even larger coordination number during the initial stage of sintering.

Exner interprets these observations with the tilting of spheres he observed in three particle models. But the cause of the separations can be interpreted in more general terms by considering the effect of particle coordination on the driving force for shrinkage, i.e., the change in free energy per unit volume:

$$\frac{dF}{dV} = \gamma \frac{dA}{dV} \quad , \tag{2}$$

where γ is the surface energy per unit area and dA/dV is the change in surface area per unit volume due to necking. Assuring that all contacting particles produce the same neck size at the same rate, then

$$\frac{dA}{dV} = ndA' \quad , \tag{3}$$

where n is the number of necks (or initial particle contacts) per unit volume and dA' is the change in area produced by a single neck. Thus, one can see that the driving force (or effective compressive stress, σ acting on the array of particles) for shrinkage is proportional to the density of necks within an array:

$$\frac{dF}{dV} = \sigma = n\gamma dA' \quad . \tag{4}$$

Since a random array of particles will contain more highly coordinated groups, these groups will have a greater driving force to shrink upon themselves relative to the total array. If the local driving force for shrinkage is greater than the average, groups that are weakly bonded together with only a few necks will separate. The tensile stress producing this separation is

$$\sigma_t = (\bar{n}-n)\gamma dA' \quad , \tag{5}$$

where $\bar{n}$ is the average neck density for the total array, and n is the higher neck density for the group.

Using this analysis, one can see that domains and agglomerates with lower than average pore coordination numbers can shrink more than the powder compact. The coordination number of the pores between these multiple particle packing units will increase during separation, and thus detrimentally alter the coordination distribution pertaining to the goal of densification.

In summary, the initial coordination distribution of a powder compact can alter during sintering. During the initial stage of sintering pores with $R < R_c$ can disappear to produce dense regions (domains and later, agglomerates) which support grain growth. As regions densify, some pull away from one another to increase the coordination number of some pores between the denser regions. During the latter stage of sintering, grain growth and/or pore size redistribution phenomena (e.g., Rayleigh instability) can decrease the coordination number of remaining pores. Since grain growth is known to occur during all stages of sintering, one might conclude that it is a dominate phenomena that reduces the coordination number of pores to values $< R_c$, and is therefore necessary to achieve theoretical density.

3.0 EXPERIMENTAL

α-Al_2O_3 powder* was dispersed in water by adjusting the pH to 2.0 with HCl and allowed to 'age' for several days. (During 'aging', the pH tended towards 4 and was periodically readjusted to 2 until only small changes were observed in a 16 hr period.) The dispersion was then mixed and allowed to sediment for a period sufficient to remove all particles > 1 μm. The resulting dispersion containing particles < 1 μm was then flocced by adjusting the pH to 9 with addition of NH_3OH. Flocculation consolidated the dispersion to ~ 15 v/o solids and prevented mass segregation due to sedimentation. Specimens were prepared for sintering/microstructure studies by casting the flocced dispersion into a cylindrical plastic mold supported on a polished, plastic plate and allowed to consolidate by evaporation.

Specimens were heated for 30 minutes at temperatures between 600°C and 1600°C. Bulk density was measured with a mercury porosimeter, which also determined the equivalent capillary diameter connecting to pore space. Microstructural changes were observed by two methods. Observations were made at the same surface location on one specimen heated incrementally between 800°C and 1600°C. Surface observations were also made after hand polishing an exterior surface with 1 μm and 1/2 μm diamond paste. An image analyzer was used to determine the area fraction and the pore size distribution on the polished surfaces.

---

* ALCOA A16 superground.

4.0 RESULTS

4.1 Bulk Density and Intrusion Capillaries

Figure 5 illustrates the bulk density vs temperature data, showing that the bulk density achieved by the evaporation-consolidation route is 0.54 ρ_t, that bulk shrinkage initiates between 1000°C and 1100°C, and that an end-point density of 0.975 ρ_t is achieved at 1500°C.

Figure 6 illustrates the mercury intrusion data. Intrusion occurs at a given pressure which, along with the assumed surface tension (484 dyn/cm^2) and contact angle (130°), determines the equivalent capillary diameter into which the mercury can fill pore space with an equivalent diameter equal or larger than the capillary size. This data results in the volume of pores interconnected by capillaries of a given size distribution.* Data in Fig. 6 shows that between 600°C and 1000°C, the pore volume connected by the larger (> 0.0925 μm) capillaries increases, whereas the pore volume connected by the smaller (< 0.0725 μm) decreases. Since the bulk density remains constant over this temperature range, pores initially associated with the smaller capillaries have redistributed to the larger capillaries. These data are in accord with Exner's[1] observations, i.e., the enlargement of pore space between more highly coordinated domains. At temperature > 1000°C, the pore volume decreases and redistribute to smaller capillaries, i.e., the larger capillaries begin to disappear.

4.2 Microstructural Observations

Polishing resulted in some surface disruption for specimens sintered at temperatures < 1200°C/30 min; observations were therefore limited to higher sintering temperatures. Figure 7 illustrates the microstructures and apparent

---

* As discussed elsewhere,[18] mercury porisometer data does not necessarily result in a pore size distribution.

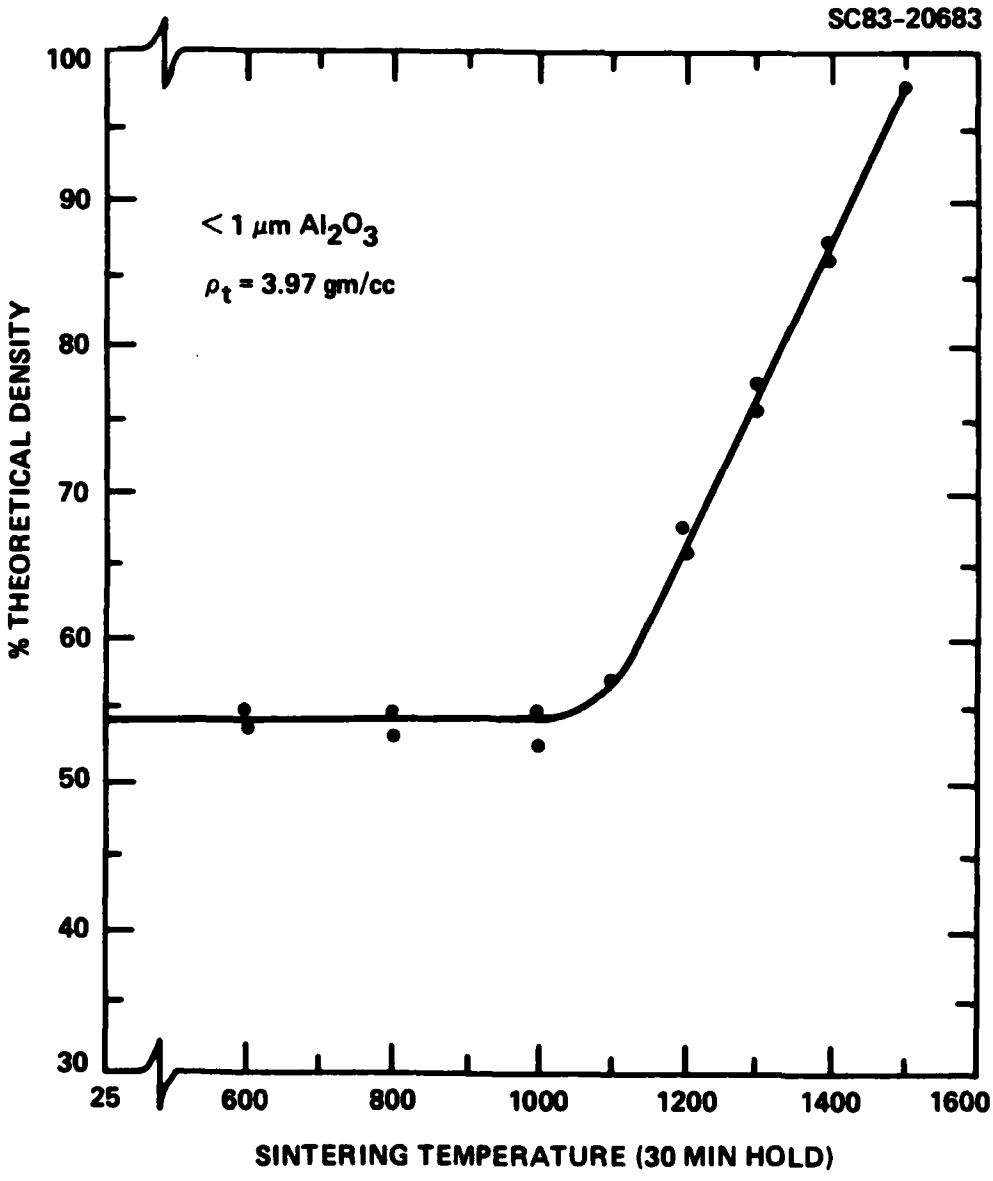

Fig. 5 Bulk density vs temperature (30 min soak) for < 1 μm α-Al_2O_3, dispersed, flocced, casted into a plastic mold and evaporated prior to heating.

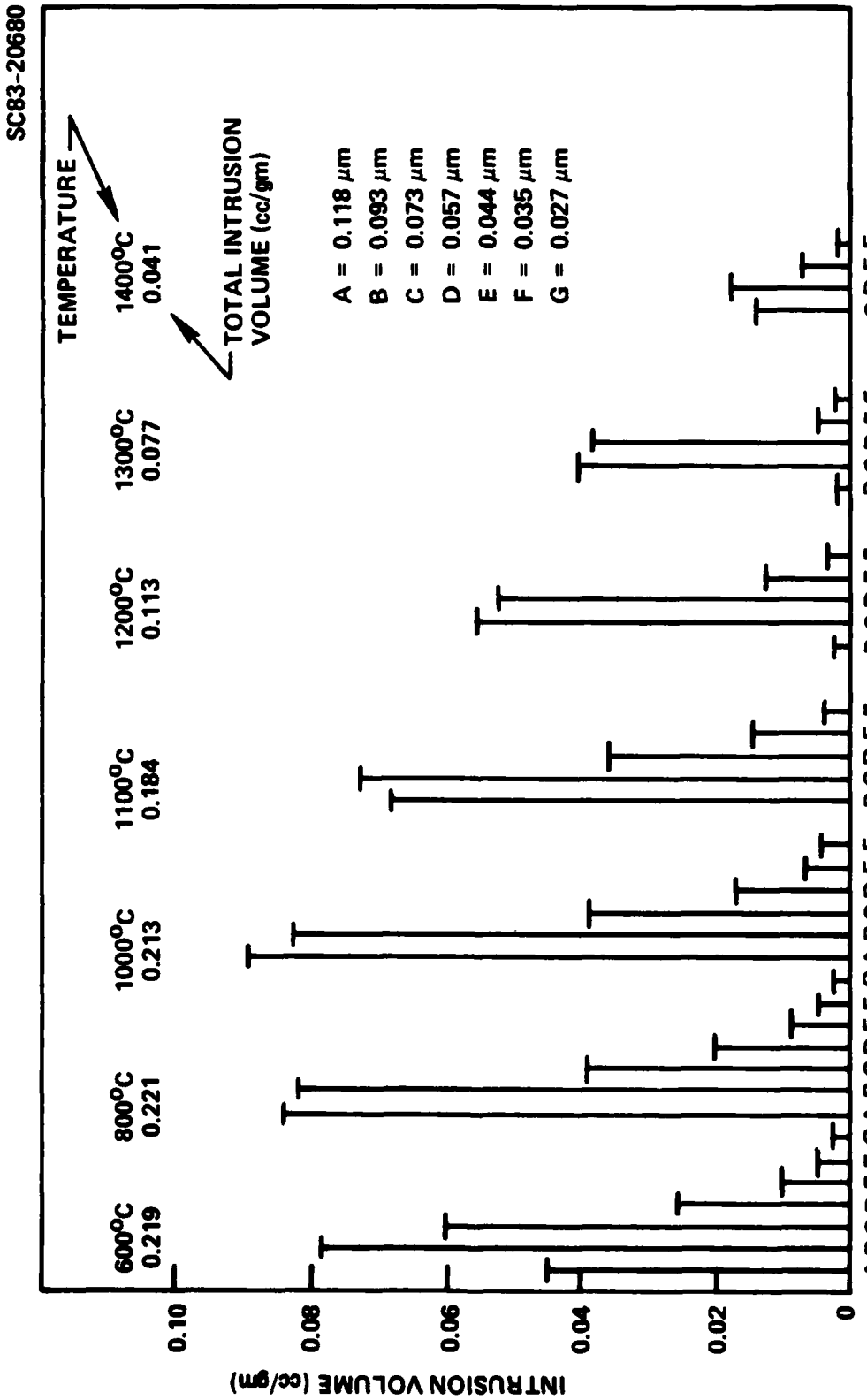

Fig. 6 Equivalent capillary size for mercury intrusion at different sintering temperatures (30 min scale) vs volume of intruded mercury.

SC83-20687

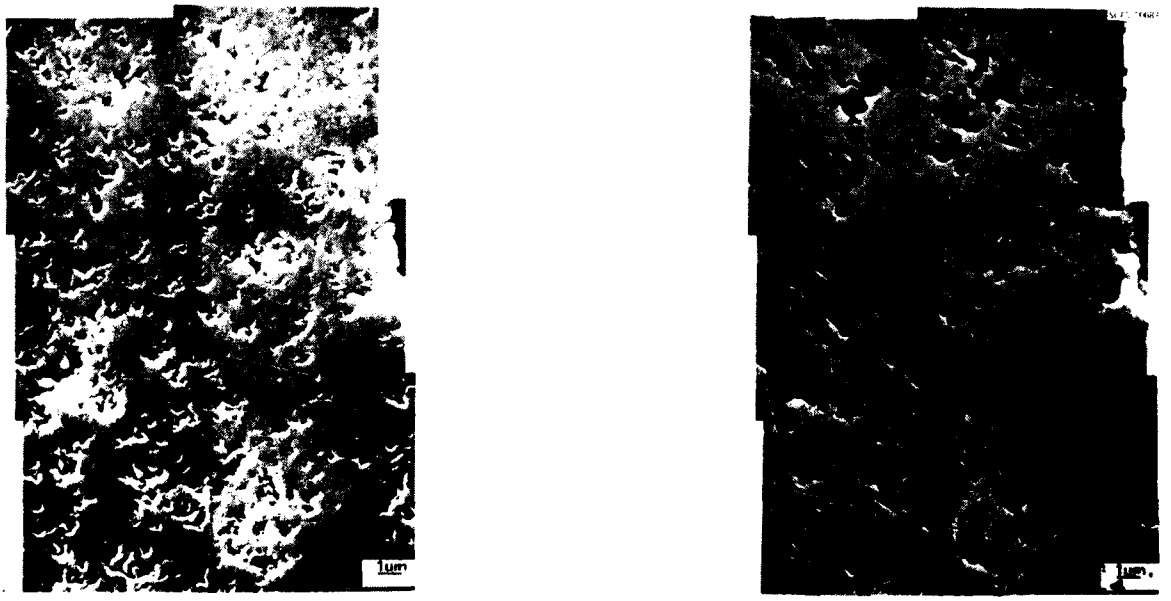

Fig. 7 Polished microstructure of < 1 μm α-Al_2O_3 sintered at 1200°C/30 min. a) polished, b) pores blanched.

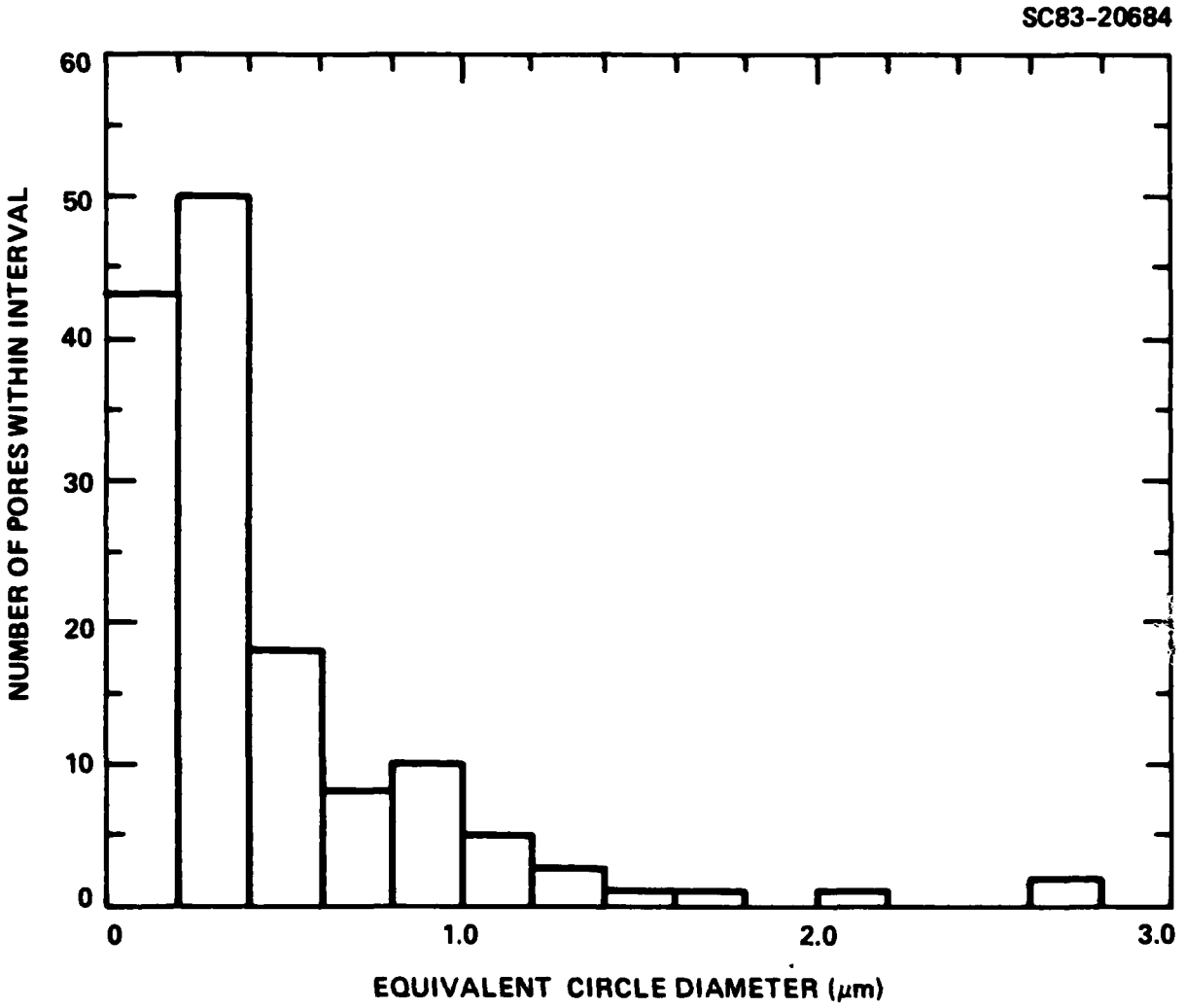

Fig. 7 Polished microstructure of < 1 μm α-Al_2O_3 sintered at 1200°C/30 min. (c) size distribution of pores.

pore size distribution observed for a specimen sintered at 1300°C/30 min. Figure 7b was produced by filling in all apparent pores with black ink on a transparent overlay. This overlay was used to determine the area fraction of the pores, and the pore size distribution with an image analyzer. The area of each pore was determined with the image analyzer and converted to an equivalent circle to derive the pore size distribution as shown in Fig. 7c.

The microstructure shown in Fig. 7 can be described as interconnecting dense regions (i.e., domains or agglomerates) 'separated' by interconnecting pores. The pore area fraction, determined with the image analyzer, was 0.24 ± 0.03, consistent with the bulk density of $0.76\ \rho_t$ as determined with the porosimeter. This correlation strongly suggests that the observed void space is representative of the whole specimen. Observations of the surface curvatures shows that most of the pores have a coordination number $> R_c$. Observations at 1100°C and 1200°C were similar in nature, except that the denser regions were smaller, and some of these regions appeared to have been pulled out by the polishing action which prevented a true representation of the pore area fraction and size distribution.

Direct observation of unpolished surfaces resulted in greater insight concerning the domains and their rearrangement. Figure 8a illustrates the array of interconnected agglomerates observed at 800°C, and Fig. 8b illustrates the size of the interconnecting domains that make up the agglomerate. The domains range from a few grains strung together as a chain to large groups that formed an irregular mass up to 1 μm in size. The domains appeared fully dense at 800°C, and were observed to support grain growth when heated to 1000°C. Most domains became single grains by 1200°C to 1300°C.

Upon reaching 1300°C, most of the pore space between the domains had disappeared, leaving dense, irregularly shaped agglomerates. The pore space between some connecting agglomerates was observed to shrink and disappear upon heating to higher temperatures, but this was not a continuous process. That is, a given interagglomerate pore could be observed to shrink, then grow before it would shrink again and disappear. Grain growth within the

SC83-20822

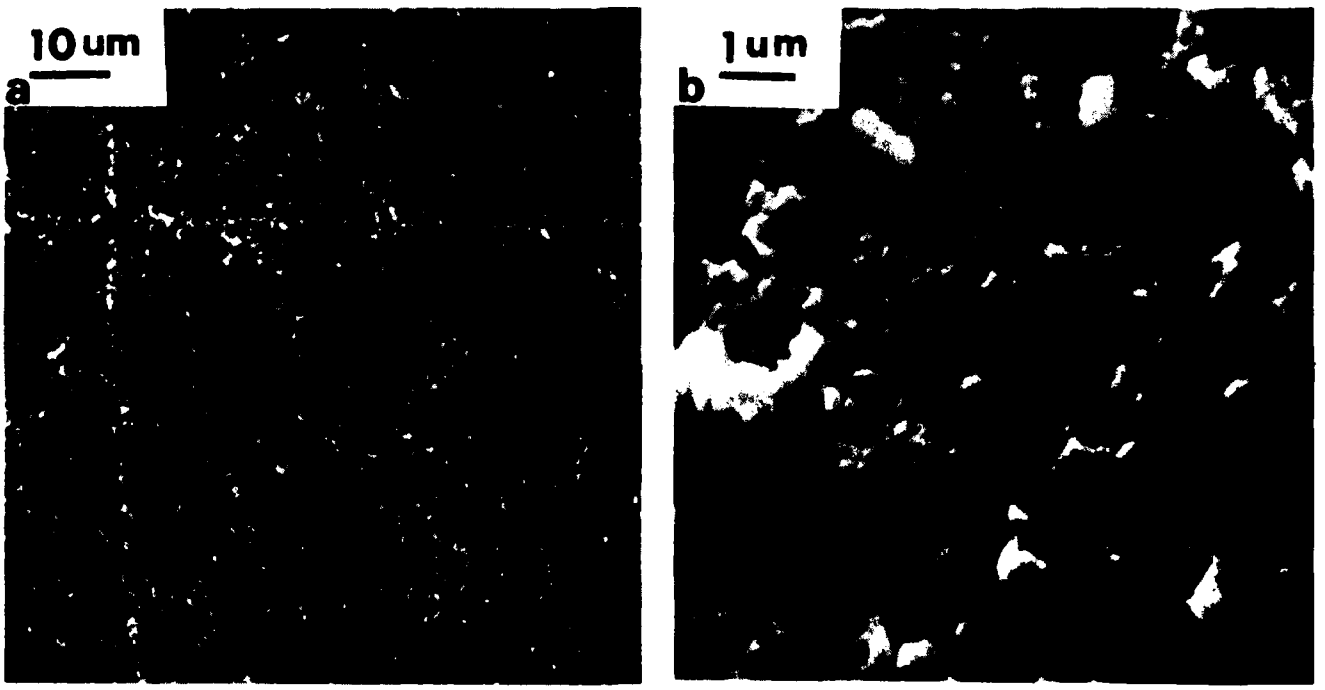

Fig. 8 Unpolished surface of < 1 μm α-Al_2O_3 sintered at 800°C/30 min: a) shows interconnected agglomerates (cross marks for relocation) and b) shows interconnected domains (see box in a).

agglomerates and agglomerate rearrangement was concurrent with interagglomerate pore growth and shrinkage. Grain growth, which initiated within domains, continued within the dense agglomerate.

Agglomerate rearrangement is illustrated in Figs. 9 and 10. Both sets of micrographs are examples taken from a 20 μm x 20 μm area which was repeatedly relocated and photographed after heat treatments initiated at 1200°C. Fig. 9 shows the disappearance of several pores with small coordination numbers (e.g., upper left corner), the formation of a new void due to rearrangement (A, 1500°C)), and the coalescence of two larger voids (B, 1550°C and 1600°C) due to the separation of two agglomerates. Note that the coordination number of voids C and B decrease due to grain growth. Voids B, with a coordination number > R_c appear to have reached an equilibrium size by 1500°C. The series shown in Fig. 10 illustrates similar phenomena, e.g., the growth of pore space between agglomerates (A), the separation of agglomerates (follow grain B as it desinters), and the closure of interagglomerate void space (follow the eventual neck formation of grains C, 1600°C). Note the change in shape of the featured agglomerate in this series as grains grow, i.e., it attempts to 'spheridize'.

Grains grew by an order of magnitude between 800°C and 1400°C, and again by nearly an order of magnitude between 1400°C and 1600°C. In all cases, dense volume elements (first domains, then agglomerates) support grain growth.

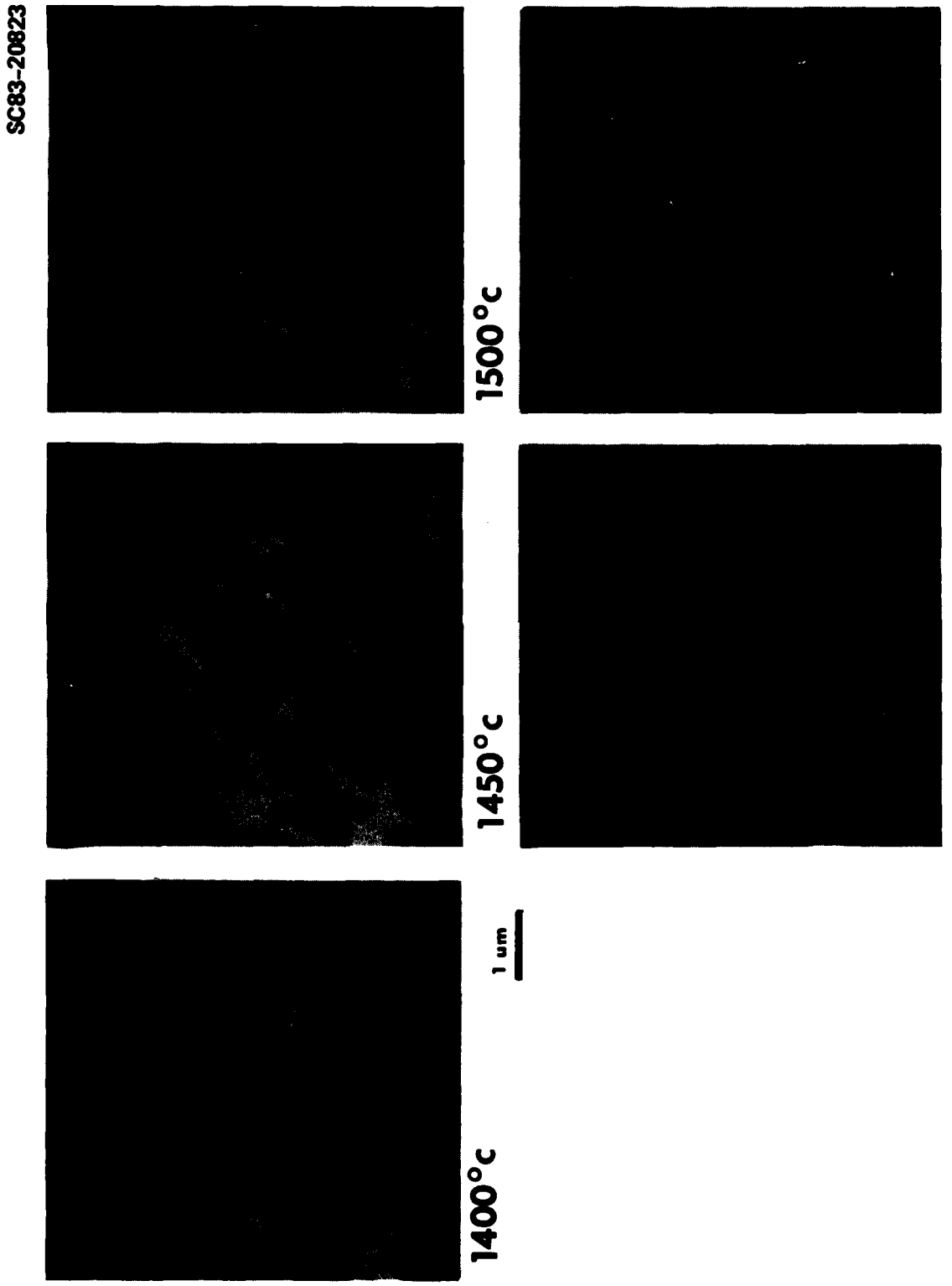

Fig. 9 Series of SEM observations of same surface area of < 1 μm Al_2O_3 sintered at temperatures indicated for 30 min.

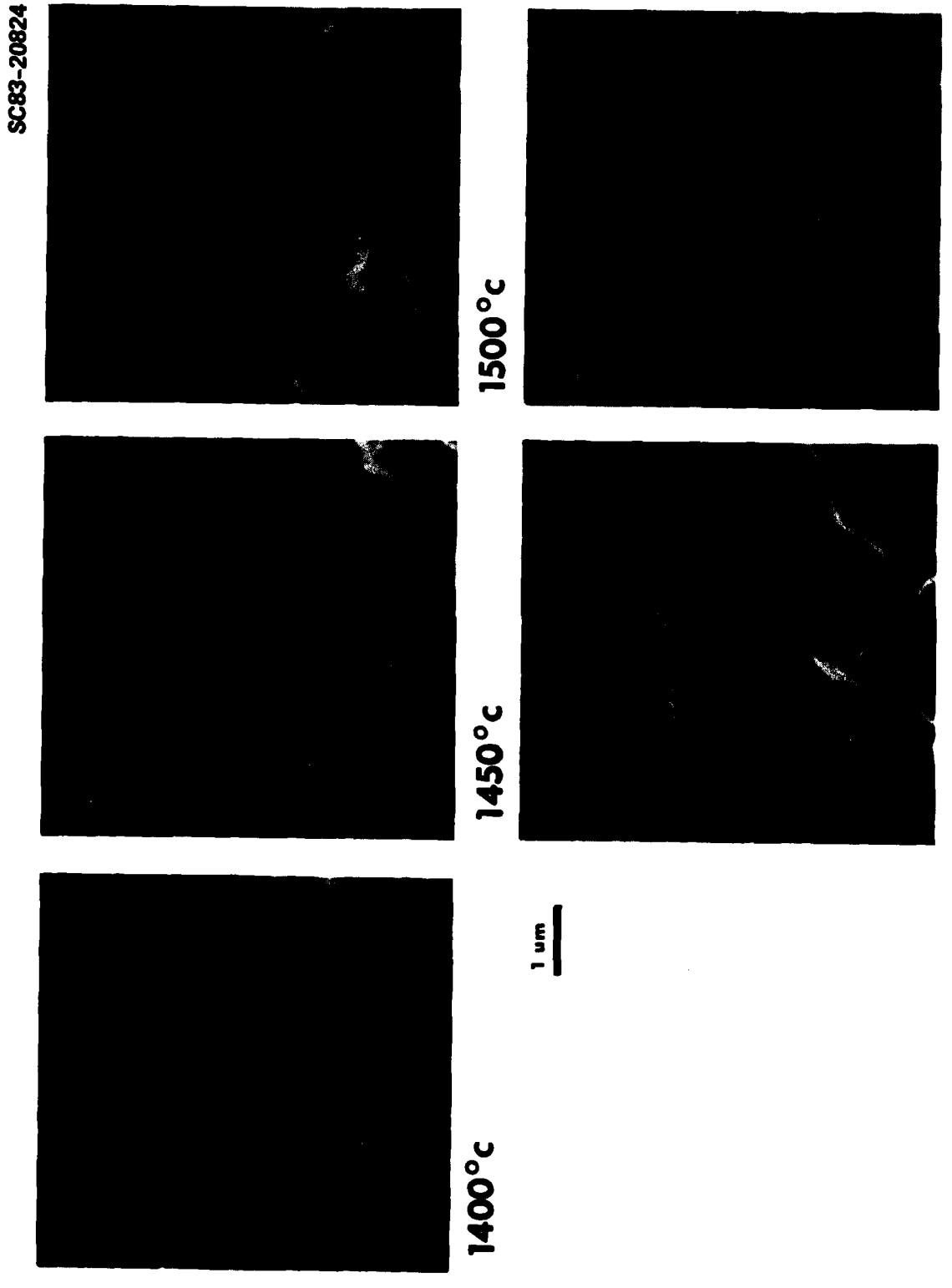

Fig. 10 (Same as Fig. 9) - Note change of agglomerate shape during grain growth.

5.0 DISCUSSION

The experimental observations strongly suggest that complete densification could have been achieved at < 1000°C if all of the pores within the powder compact had the same coordination distribution as the domains. In reality, the powder packed as domains and agglomerates to produce pores with much higher coordination numbers. During heating to 1000°C, domains densified and seperated to increase the size and coordination number of the interdomain pores. This process occurred with no apparent shrinkage. Subsequent heating to ~ 1300°C reduced the average coordination number and size of the interdomain pores by grain growth and the rearrangement process, respectively. This resulted in the disappearance of interdomain pores to form dense agglomerates and shrinkage. Interagglomerate pores disappear by similar processes upon further heating to 1600°C. Some interagglomerate pores remained at 1600°C to result in an end-point density slightly less than theoretical.

It might be concluded that grain growth and rearrangement processes are the two phenomena that control the densification of an agglomerated, powder compact. The role of grain growth has already been discussed, viz. to decrease the coordination number.* The role of rearrangement is two-fold. First, interconnecting packing units that have more contacts per unit volume than the average (domains and later, agglomerates) shrink faster than the compact as a whole to produce fissures. As discussed, this rearrangement process is detrimental to densification. Second, rearrangement also appears to produce new contacts at a later stage to help close fissures. This rearrangement process is advantageous to densification. It is obvious that an external compressive stress would greatly increase this rearrangement process. One can only conclude that the true role of hot-pressing is to aid

---

* It is also obvious that agglomerates can initiate exaggerated grain growth. Namely, since dense agglomerates support grain growth, a large agglomerate can initiate unwanted, exaggerated grain growth.

advantageous rearrangement to minimize the development of fissures. If fissures are prevented, grain growth is not required to reduce the coordination number.

Lacking an externally applied pressure, the question is, what are the mechanisms that produce advantageous rearrangement? Although an answer is not clear, several might be listed: 1) the effective compressive stress exerted on the compact as a whole as indicated by Eq. (4), 2) the 'spheridization' of the domains and agglomerates that occurs during grain growth, and 3) the rearrangement of narrow pore spaces due to surface (Rayleigh) instability. Whatever the mechanism(s), it is obvious that the kinetics of rearrangement will depend on the ability of the dense regions to deform. This would be an interesting and significant research area for further understanding the kinetics of sintering.

Acknowledgements

The author is grateful to B.I. Davis who performed the sintering and posisimeter work. Discussions with Drs. I. Aksay, P.E.D. Morgan and D.R. Green were invaluable. This work was supported by the Office of Naval Research under Contract No. N0004-82-C-0341.

6.0 REFERENCES

1. H.E. Exner, "Principles of Single Phase Sintering," Reviews on Powder Metallurgy and Physical Ceramics, 1 [1-4], p. 1-251 (1979).

2. K. Haberko, "Characteristics and Sintering Behavior of Zironic Ultrafine Powders," Ceramics International, 5, 148 (1979).

3. D.E. Niesz and R.B. Bennett, "Agglomerate Structure and Properties," Ceramic Processing Before Firing," Ed by G.Y. Onoda, Jr., and L.L. Hench, John Wiley (1978).

4. J.S. Reed, T. Carbone, C. Scott and S. Lukasiewicz, "Some Effects of Aggregates and Agglomerates in the Fabrication of Fine Grained Ceramics," Processing of Crystalline Ceramics Ed by H. Palmour III, R.F. Davis and T.M. Hare, p. 171-80, Plenum (1978).

5. C.A. Bruch, "Sintering Kinetics for the High Density Alumina Process," Bull Am. Ceram. Soc. 41, 799 (1962).

6. W.D. Kingery and B. Francois, "Sintering of Crystalline Oxides, I. Interactions Between Grain Boundaries and Pores," Sintering and Related Phenomena Ed. by G.C. Kuczynske, N.A. Hooton, and G.F. Gibbon, p. 471-98, Gondon Breach (1967).

7. R.M. Cannon, "The Effects of Dihedral Angle and Pressure on the Driving Forces for Pore Growth and Shrinkage," to be published.

8. J.D. Bernal, "The Bakerian Lecture, 1962: The Structure of Liquids," Proc. R. Soc. 280A, 299 (1964).

9. H.J. Frost, "Overview 17: Cavities in Dense Random Packing," Acta Met 30 [5] p. 889-904 (1982).

10. R.K. McGeary, "Mechanical Packing of Spherical Particles," J. Am. Ceram. Soc. 44 [10], 513 (1961).

11. T.G.M. van de Ven and R.J. Hunter, "Energy Disappation in Sheared Coagulated Sols," Rehologic Acta 16 [5], 534-43 (1977).

12. G.D. Scott, A.M. Charlesworth and M.K. Mak, "On The Random Packing of Spheres," J. Chem. Phys. 4, 611 (1964).

13. T. Vasilos and W. Rhodes "Fine Particulates to Ultrafine-Grain Ceramics," Ultrafine Grain Ceramics, Ed. by J.J. Burke, N.L. Reed and V. Weiss, p. 137-172, Syracuse University Press, 1970.

14. T.K. Gupta, "Possible Correlation Between Density and Grain Size During Sintering," J. Am. Ceram. Soc. 55 [5] 276 (1972).

15. T.K. Gupta, "Crack Healing in Thermally Shocked MgO," J. Am. Ceram. Soc. 58 [3-4] 143 (1975).

16. C.F. Yen and R.L. Coble, "Speroidization of Tubular Voids in Al_2O_3 Crystals at High Temperatures," J. Am. Ceram. Soc. 55 [10] 507 (1972).

17. O.J. Whittemore, Jr. and J.J. Sipe, "Pore Growth During The Initial Stages of Sintering Ceramics," Powder Tech. 9, 159 (1974).

18. F.F. Lange and B.I. Davis to be published.